J. Anat. (2005) **207**, pp283–295

REVIEW

Facial surface analysis by 3D laser scanning and geometric morphometrics in relation to sexual dimorphism in cerebral–craniofacial morphogenesis and cognitive function

Robin J. Hennessy,[1] Stephen McLearie,[1,2] Anthony Kinsella[1,3] and John L. Waddington[1]

[1]*Stanley Research Unit, Department of Clinical Pharmacology, and Research Institute, Royal College of Surgeons in Ireland, Dublin, Ireland*
[2]*Department of Child and Adolescent Psychiatry, St James's Hospital, Dublin, Ireland*
[3]*School of Mathematics, Dublin Institute of Technology, Dublin, Ireland*

Abstract

Over early fetal life the anterior brain, neuroepithelium, neural crest and facial ectoderm constitute a unitary, three-dimensional (3D) developmental process. This intimate embryological relationship between the face and brain means that facial dysmorphogenesis can serve as an accessible and informative index of brain dysmorphogenesis in neurological and psychiatric disorders of early developmental origin. There are three principal challenges in seeking to increase understanding of disorders of early brain dysmorphogenesis through craniofacial dysmorphogenesis: (i) the first, technical, challenge has been to digitize the facial surface in its inherent three-dimensionality; (ii) the second, analytical, challenge has been to develop methodologies for extracting biologically meaningful shape covariance from digitized samples, making statistical comparisons between groups and visualizing in 3D the resultant statistical models on a 'whole face' basis; (iii) the third, biological, challenge is to demonstrate a relationship between facial morphogenesis and brain morphogenesis not only in anatomical–embryological terms but also at the level of brain function. Here we consider each of these challenges in turn and then illustrate the issues by way of our own findings. These use human sexual dimorphism as an exemplar for 3D laser surface scanning of facial shape, analysis using geometric morphometrics and exploration of cognitive correlates of variation in shape of the 'whole face', in the context of studies relating to the early developmental origins of schizophrenia.

Key words brain dysmorphogenesis; craniofacial dysmorphogenesis; facial development; neuropsychology; schizophrenia.

Introduction

A primary characteristic by which humans present themselves to the external world is via the anatomy of their facial shape. This influences the subjective perception of a given person by another person, for example in terms such as 'attractive' or 'distinguished'. However, facial shape and its morphogenesis can also inform on each person's biology through variation therein and, in more marked instances, in terms of clinical dysmorphology. This can reveal fundamental aspects of the pathobiology of disease through underlying dysmorphogenesis and has the greatest potentiality in relation to neurological and psychiatric disorders of early developmental origin; for example, craniofacial dysmorphology occurs not only in major chromosomal abnormalities such as Down's syndrome (Allanson et al. 1993) but also in less readily recognizable conditions such as velo-cardiofacial syndrome (Murphy & Owen, 2001) and, to an even more subtle, quantitative extent, in schizophrenia

Correspondence
Professor John L. Waddington, Department of Clinical Pharmacology, Royal College of Surgeons in Ireland, St Stephen's Green, Dublin 2, Ireland. T: +353 1 402 2245; F: +353 1 402 2453; E: jwadding@rcsi.i.e.

Accepted for publication *9 June 2005*

(Lane et al. 1996, 1997; Waddington et al. 1999a,b; McGrath et al. 2002; Hennessy et al. 2004).

Specifically, facial dysmorphology occurs in these and potentially other neuropsychiatric disorders of early developmental origin because the face and anterior brain emerge and evolve in exquisite embryological intimacy; indeed, over early fetal life the anterior brain, neuroepithelium, neural crest and facial ectoderm constitute a unitary, three-dimensional (3D) developmental process (Diewert & Lozanoff, 1993a,b; Diewert et al. 1993; Kjaer, 1995; Waddington et al. 1999a,b; Schneider et al. 2001; Baldwin et al. 2004). Hence disruption to brain morphogenesis is accompanied by facial dysmorphogenesis. In a complementary manner, disruption to facial morphogenesis is accompanied by brain dysmorphogenesis; for example, individuals with cleft lip/palate are characterized anatomically by abnormalities of brain structure on magnetic resonance imaging (MRI) (Nopoulos et al. 2002a) and functionally by cognitive deficits on neuropsychological testing (Nopoulos et al. 2002b).

Such dysmorphology in neuropsychiatric disorders has long been described on a clinical basis through inspection of individual patients, either impressionistically or with subjective observations 'operationalized' using a checklist such as the Waldrop scale (Waldrop et al. 1968). This has been supplemented by anthropometric techniques involving direct linear measurements made between classical craniofacial landmarks, but a fundamental omission is apparent: development is an inherently 3D process, and hence any approach which fails to capture this dimensionality anatomically loses critical information that can inform powerfully on the underlying developmental pathobiology. Trigonometrical techniques for quantifying craniofacial and cerebral configurations in 'pseudo-3D' have been introduced for *in vitro* archival material such as the Carnegie embryological collection (Diewert & Lozanoff, 1993a,b; Diewert et al. 1993) but these use only a small fraction of the available anatomical information. We have described an interim approach for determining in living subjects simple 3D configurations from the unique subset of linear measurements that define the unambiguous space encompassed by those measurements (Hennessy et al. 2004), but again these use only a limited amount of the available anatomical information.

There are thus three principal challenges to this approach to increasing understanding of disorders of early brain dysmorphogenesis through craniofacial dysmorphogenesis: (i) the first, technical, challenge has been to digitize the 'whole' facial surface in its inherent three-dimensionality; (ii) the second, analytical, challenge has been to develop methodologies for extracting biologically meaningful shape covariance from digitized samples, making statistical comparisons between groups and visualizing in 3D the resultant statistical models; (iii) and the third, biological, challenge is to show that variation in facial morphology reflects variation in adult brain function. Here we consider each of these challenges in turn and then illustrate the issues further by way of our own findings from studies relating to the early developmental origins of schizophrenia.

Digitisation technologies for capturing the facial surface

Surface digitization technologies have emerged on an experimental basis over the past 20 years but commercial systems based on several optical principles are now becoming increasingly available for a variety of biological/anatomical applications.

Two technologies are commonly employed for digitizing the facial surface, namely laser scanning and photogrammetry. In laser scanning, the face is traversed by a laser light source. Digital cameras monitor the illumination and triangulation geometry allows depth information to be calculated; the light source can be a point or plane and the face can be moved through the light source or vice versa. This technology generally produces facial surfaces with accuracy and resolution of ~1 mm and can take up to 30 s. Some systems require a trained operator to acquire optimal facial scans while others are automated. In photogrammetry, the face is illuminated by either a structured or a speckled light pattern and images are recorded simultaneously from several views. Then, images are post-processed to calculate facial surface coordinates. The main advantage of photogrammetry is its speed of data capture, typically less than 1 s. Commercial photogrammetric systems vary in their performance and disadvantages of individual systems include lengthy post-processing times, surface artefacts and uneven surface coverage. Accuracies are typically ~0.5 mm. Both laser scanning and photogrammetric systems vary considerably in their portability. Our own work has focussed on 3D laser surface scanning of the face (Hennessy et al. 2002). We employ a portable hand-held laser scanner, FastSCAN (Polhemus FastScan, Polhemus Inc, VT, USA). This

combines laser triangulation optics (laser line and two cameras) with Polhemus 3Space tracking technology; two sensors, one attached to the optics and another to a headband, are used to track both the position of the optics and movement of the subject's head. Technical details are available at www.fastscan3d.com. The face is recorded typically in ~30 s. After initial instruction and training, scans of even resolution across the face can be produced. Resolution and accuracy are ~1 mm. The main advantages of this system are its portability and ease of use to generate smooth scans with all facial features recorded in detail. The main disadvantages of the system are its sensitivity to light and to metal objects, requiring careful control of its operating environment, and the speed of data capture which makes it less suitable for scanning younger children.

Analytical and visualization techniques

Extraction of biologically important information on shape covariance from digitized samples has been developed as geometric morphometrics, which has now found extensive applications to human data, both anatomical and clinical. Geometric morphometrics is applied to sets of landmark coordinate [*x*, *y*, *z*] values. The coordinates are transformed to remove size, location and orientation, and the set of transformed coordinates is treated as a single point in a multivariate shape space. The results are statistically robust and can be visualized to provide information on the anatomical origin of statistical parameters at issue. Reviews of this approach for biological practitioners are available (O'Higgins & Jones, 1998); Dryden & Mardia (1998) provide a formal exposition. Applications to face and brain studies include facial anthropology (Bookstein et al. 1999; Weber et al. 2001; Hennessy & Stringer, 2002), facial growth (Dean et al. 2000; Hennessy & Moss, 2001; Penin et al. 2002; Hutton et al. 2003), facial syndromes (Hammond et al. 2004), fetal alcohol syndrome (Bookstein et al. 2001), clinical malocclusion (Singh et al. 1997), sexual dimorphism (Hennessy et al. 2002), brain pathology in schizophrenia (DeQuardo et al. 1996; Tibbo et al. 1998; Buckley et al. 1999; Gharaibeh et al. 2000) and facial dysmorphology in schizophrenia (Hennessy et al. 2004).

However, a shortcoming of much of this early work in the field was that the 3D surface between landmarks could not be interrogated and thus important and potentially critical information was lost to analysis. Recently, new approaches have been developed, including sliding [semi] landmarks and interpolated [pseudo] landmarks that allow for approximations to analysis of the whole facial surface. These now constitute an important research front in morphometrics.

Semi-landmarks are points lying along a curve between two landmarks that are allowed to slide along the curve until a geometric parameter (bending energy) is minimized (Bookstein, 1997a). This is a promising approach that has been developed primarily in relation to 2D data, for example in studies of the corpus callosum and subcortical brain structures in fetal alcohol syndrome (Bookstein et al. 2001) and of the corpus callosum in schizophrenia (Bookstein, 1997b). By contrast, pseudo-landmarks are points that are interpolated between landmarks. In 2D they lie along curves and in 3D along surfaces. An important application of pseudo-landmarks is in the generation of landmark sets on which active shape models are based (Hill et al. 1996). In 3D, an elegant interpolation method, which uses 3D thin plate splines, has recently been applied to facial surfaces (Hutton et al. 2003) and our approach, described in detail below, is based on these 3D splines.

There is currently a disparity between technical advances in acquiring surface data and analytical advances in processing statistically and then visually the data so acquired.

Facial morphology and brain function

Although the intimate relationship between facial morphogenesis and brain morphogenesis is well established embryologically, it would be an important additional validation of this approach if it could be shown that variation in facial morphology reflects variation in adult brain function. The requirements for investigating any such relationships are: an appropriate surface digitization technology that can be applied readily to human subjects; and elaboration of geometric morphometric techniques to allow analysis of the covariant relationship of facial shape parameters, preferably on a 'whole-face' basis, to any phenotypic measure in those subjects. To our knowledge, there are not yet any studies of this type.

One readily accessible index of brain function is cognition. This is assessed neuropsychologically and typically generates measures as continuous variables. The determination of their covariance with facial shape corresponds, analytically, to the commonly studied

relation of shape to size, i.e. allometry. Geometric morphometric studies of allometry include a primate study (O'Higgins & Jones, 1998) and a comparison of human and chimpanzee onotogenetic paths (Penin et al. 2002). These provide the methodological basis for the studies that we have undertaken to relate facial shape to cognitive function.

Human sexual dimorphism and its cognitive correlates as an exemplar

Methodological approaches: morphology

Subjects

Our studies involved 128 otherwise unselected members of staff of the Royal College of Surgeons in Ireland [82 females: age 32.2 years (SD 9.2), range 20–59 years; 46 males: age 33.1 years (SD9.7), range 22–65] (see Hennessy et al. 2002). Following approval by the Research Ethics Committee of the Royal College of Surgeons in Ireland, the subjects gave written, informed consent to their participation in the study. To ensure ethnic homogeneity regarding evident ethnic differences in facial shape, all subjects were of Irish, Scottish, Welsh or English origin, as were their parents.

3D laser surface scanning

The laser scanner hardware has been described above. The captured data consist of a dense cloud of points that spans the facial surface. These are processed to generate a single surface mesh, i.e. 3D coordinate vertices arranged as triangular facets; this is to allow the points to be visualized by computer graphics. The density of the surface mesh is determined by surface fitting parameters that are set by the operator. A typical high-resolution surface, consisting of ~80 000 vertices and ~200 000 triangular facets, is shown in Fig. 1.

Extraction of landmarks

Twenty-six landmarks, marked A–Z in Fig. 1, were located by the same investigator. The first 24, marked A–X in Fig. 1, were used in the landmark analysis and have been described previously in detail (Hennessy et al. 2002). The full 26-landmark set, consisting of these 24 landmarks plus right and left otobasion inferius, was used in the generation of pseudo-landmarks as described below.

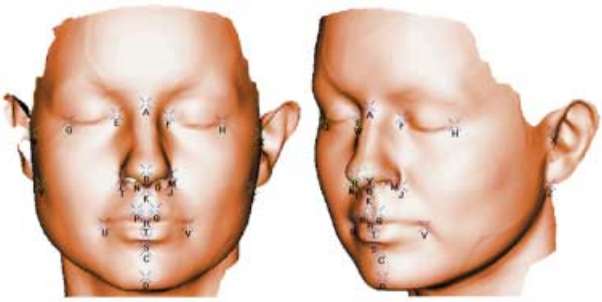

Fig. 1 High-resolution surface with 26 landmarks, marked A–Z. Landmarks A–X are as described previously (Hennessy et al. 2002); landmarks Y and Z are right and left otobasion inferius.

Generation of pseudo-landmarks

The method for the generation of pseudo-landmarks is a development from that described by Hutton et al. (2003). In brief, a surface mesh is used as a template for locating pseudo-landmarks in each of a set of surface scans. Our method consists of seven straightforward steps:

1 A set of facial surface scans is assembled. Facial scans are excluded if they have significant holes and/or substantial facial hair.

2 For each of the surface scans a high-resolution surface mesh is created, which consists of typically 80 000 vertices, as described above. The 26 landmarks are manually located on these.

3 One of the surface scans is selected to have even coverage over the facial surface, without holes or artefacts and a superior border low on the forehead. A low-resolution base mesh is generated from it. Base meshes are edited to remove ears and, where necessary, regions below the mandible, in order to produce a facial surface of minimal coverage.

4 Each individual high-resolution surface is warped onto the base mesh using 3D thin plate splines and the 26 landmarks as control points. For each vertex on the base mesh the point of correspondence on the high-resolution surface is located, to a close approximation, as the nearest vertex. The coordinates of the vertices on the unwarped surface plus the coordinates of the 26 landmarks constitute the [approximate] pseudo-landmark set. These pseudo-landmark sets represent the intersection of the high-resolution surface and the base mesh and, because the high-resolution surfaces are more extensive than the base mesh, the coverage of the pseudo-landmarks corresponds to that of the base mesh.

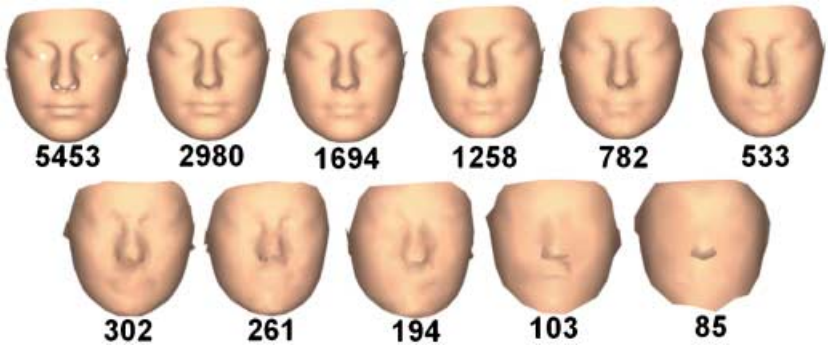

Fig. 2 Surfaces based on each of the 11 pseudo-landmark sets. Numbers below each image indicate the number of coordinates in each pseudo-landmark set.

5 Generalize Procrustes analysis (Goodall, 1991) is applied to the pseudo-landmark sets and the Procrustes mean is calculated.

6 Each high-resolution surface is warped onto the Procrustes mean using thin plate splines and the 26 landmarks as control points. For each vertex on the base mesh, the closest facet on the surface is located. The vertex is projected onto the plane defined by the facet and the barycentric coordinates of the projected point with respect to the facet coordinates are calculated. The coordinates of the equivalent point on the unwarped surface are then calculated from the barycentric coordinates. These coordinates plus the coordinates of the 26 landmarks constitute the final pseudo-landmark set.

7 The connectivity of the base mesh is transferred to the pseudo-landmark set and the extra 26 landmarks are added to the mesh. The output is the set of pseudo-landmark coordinates plus their connectivity mesh.

This method is a simple but effective technique for calculating points of correspondence on facial surfaces. The two-pass approach ensures that the outcome is unaffected by choice of subject for the initial base mesh. The thin plate spline interpolations ensure that each surface is smoothly warped onto the base mesh and the choice of the Procrustes mean as base mesh in the second pass ensures that the amount of warping is minimized.

The calculation times ranged from 305 s for the highest resolution base mesh to 20 s for the lowest on a 350-MHz personal computer.

Validation with conventional landmark analysis

Pseudo-landmark sets were generated with 11 base meshes, ranging from 5453 to 85 vertices. These correspond to mean intervertex distances of 2.7 and 24.6 mm, respectively. The absolute values of mesh sizes are not critical but the range of resolutions was selected such that at the lowest resolution the main facial features were barely recognizable while at the highest resolution the facial features were rendered with a high level of detail, as shown in Fig. 2.

The pseudo-landmark and landmark sets were analysed following the geometric morphometrics paradigm that we have previously described in detail (Hennessy et al. 2002). In outline:

1 *Shape space coordinates*. The pseudo-landmark and landmark sets were transformed via Generalized Procrustes Analysis to eliminate scale, location and orientation. Each transformed set then constitutes a point in a shape space. Because the dimensionality of this space is high, ranging from 65 for the landmark set to 248 for the low-resolution set to 16 352 for the high-resolution set, it must be reduced for statistical tests to have sufficient power. The dimensionality was reduced via Principal Component (PC) analysis, which enables most of the shape variance to be captured by a relatively small number of variables. The Eckart–Young theorem (Johnson, 1963) was used to generate 128 eigenvectors and the Procrustes residuals, which were projected onto the eigenvectors to generate PC scores. The PC scores, eigenvalues and eigenvectors were written out for statistical analysis and visualization.

2 *Analysis of discrimination*. Hotelling's T^2 test, a parametric multivariate test of group difference, was applied to the first 18 PC scores; the number of PC scores was determined as those PCs entered into logistic regression analysis, in most cases, using a standard criterion described below. This test also generates a distance measure, Mahalanobis D^2, which was recorded. For the landmark sets, Goodall's *F*-test (Goodall, 1991; Bookstein, 1997a), a well-established and powerful (Rohlf, 2000) test for overall shape difference between two groups, was also applied.

3 *Model of discrimination*. In order to localize significant group differences, logistic regression was carried out with gender as the dependent variable and PCs as the independent variables to establish which PCs of shape contributed to shape discrimination by gender. PCs with eigenvalues greater than the mean, a standard selection criterion used in previous work, were included. A parsimonious regression model was produced using a forward stepwise procedure. R^2 values were calculated using the ordinary least-squares method (Menard, 2000).
4 *Visualisation*. The parsimonious regression models were visualized by multivariate regression of the significant shape PCs onto the predicted values for gender. The β coefficients of the model, which have the units of shape/gender, were visualized by adding appropriately weighted eigenvectors to the Procrustes mean (Penin et al. 2002). This causes the coordinate of each point of the Procrustes mean to be displaced and thus the mean face to be warped along the male–female discrimination axis. The warping was done dynamically with multiple views to aid appreciation of the shape change.

In addition, the following numerical information was added by colour coding to the resultant 3D graphics. (i) Displacement vector length, direction and projections perpendicular and parallel to the surface were colour coded as continuous variables or percentiles; inward or outward displacements were coded as blue or red, respectively. (ii) Facet area change was coded as continuous, percentile or binary variables; increases or decreases in facet area were coded as red or blue, respectively.
5 *Ordination*. Ordination along the male–female axis was computed using discriminant function analysis; the same PCs were used as for the logistic regression and discriminant function scores were calculated. The ordinations for pseudo-landmark and landmark sets were compared by computing Pearson coefficients for correlations between the linear discriminant function scores for the highest resolution surface and each of the other surfaces.

Morphological findings

Statistical analysis of sexual dimorphism in human facial shape

Omnibus testing
For all 'whole-face' and 24-landmark analyses, Hotelling's T^2 was significant ($P < 0.001$). The values of Mahalanobis D^2, a measure of the shape distance between the two groups, are plotted in Fig. 3. Mahalanobis D^2 increases rapidly from the value for the 24-landmark analysis and reaches a plateau for pseudo-landmark sets consisting of ~200 coordinates. Inspection of the surfaces (Fig. 2)

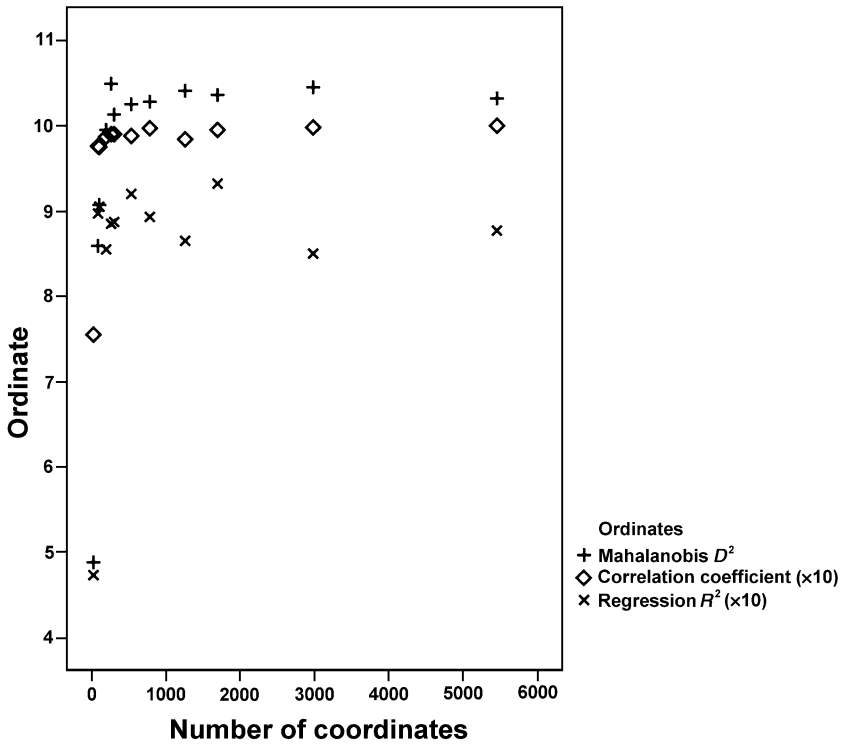

Fig. 3 Mahalanobis D^2, logistic regression R^2 (×10) and correlations between the linear discriminant function scores for the highest resolution surface and each of the other surfaces (×10), in relation to size of pseudo-landmark/landmark set as number of coordinates.

shows that at this resolution there is initial delineation of the mouth and nose; this delineation is heightened as the number of coordinates increases.

Regression modelling

R^2 values for the logistic regression models are plotted in Fig. 3. R^2, indicating the extent of the association, rises steeply from the value for the 24-landmark analysis and reaches a plateau around the same surface resolution as for Mahalanobis D^2.

Visualisation

In Fig. 4, visualizations are presented for the discriminant function that transforms the Procrustes mean along the male–female axis by adding a displacement vector to each point on the facial surface; visualizations are generated from the highest resolution surface (5453 coordinates) and presented in coronal, oblique and sagittal planes. The Procrustes mean coordinates are depicted, with equal displacements in each direction along the male–female discrimination axis. These correspond to exaggerating male–female dimorphism approximately three-fold for clarity. The displacement vectors for each point of the female surface are also represented in Fig. 5, colour coded to represent the length of the displacement vector at each point, the angle of the displacement vector to the surface normal and the change in (local) surface area. The colour coding is a subset of the coding options that contains most of the coded information. The overall male–female transformation is best understood by examining the colour-coded images simultaneously, along with dynamic 3D graphics.

Anatomy of sexual dimorphism in human facial shape

The graphics provide a detailed and informative depiction of the geometric representation of the statistically significant male–female discrimination model (R^2 = 85.3%); this consists of seven significant shape PCs which constitute the parsimonious regression model: PC 2 ($P < 0.001$), PC 4 ($P < 0.005$), PC 5 ($P < 0.005$), PC 6 ($P < 0.005$), PC 9 ($P < 0.001$), PC 10 ($P < 0.05$) and PC 11 ($P < 0.001$). These show that in general terms the face is divided into two primary domains: a medial region and lateral mandibular region, which moves inwards, and the rest of the face, which moves outwards with increasing 'femaleness'. The colour coding for vector

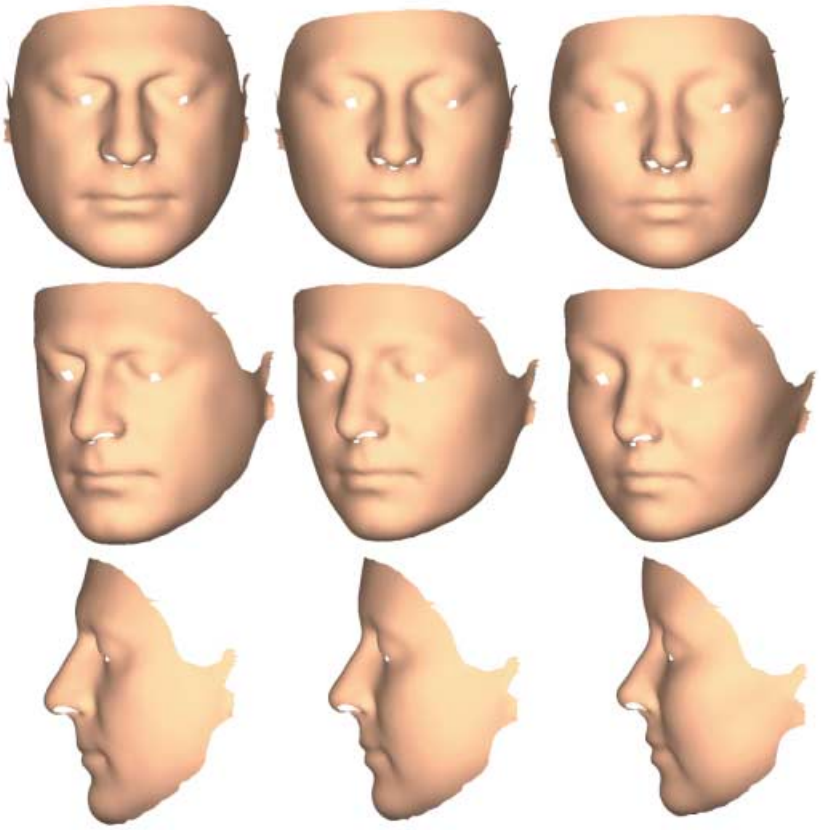

Fig. 4 The Procrustes mean (middle column) displaced equally in each direction along the male–female discrimination axis in female (right column) and male (left column) directions. The displacement positions of the male and female faces correspond to the male–female dimorphism exaggerated approximately three-fold. The highest resolution surface is shown.

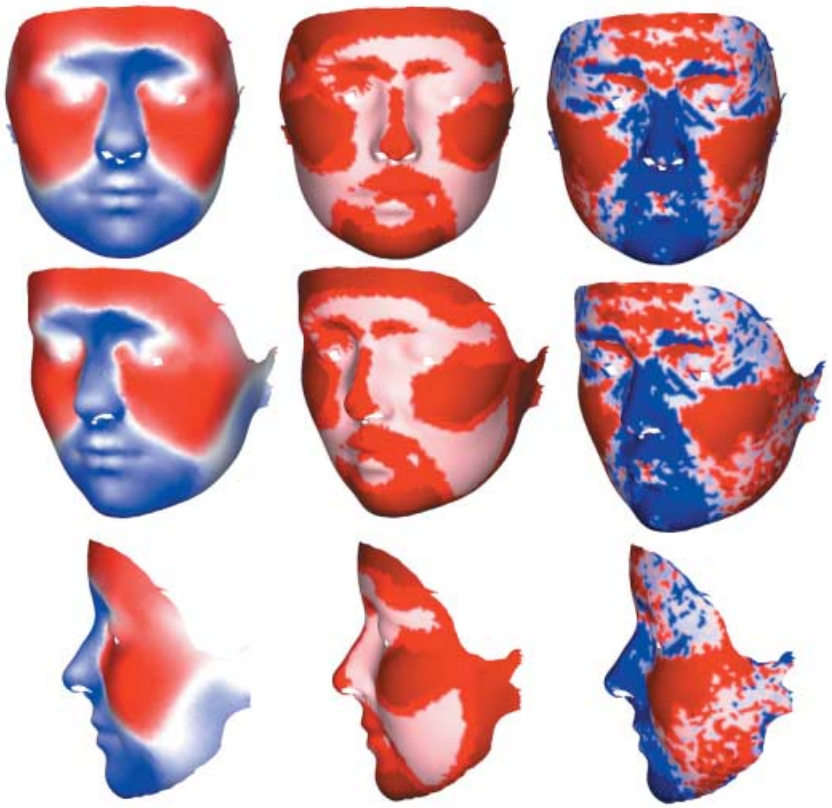

Fig. 5 The displacement vectors for each point of the female surface colour coded. Left column: the angle of the displacement vector to the surface normal is coded as red (outwards) or blue (inwards), with stronger colours coding smaller angle to the normal, i.e. displacement vector more normal to the surface. Middle column: the relative length of the displacement vector at each point colour coded as 33% percentiles, with the darker colours coding the upper percentiles. Right column: the change in (local) surface area coded as red (increase) or blue (decrease) and coded as 33% percentiles, with the darker colours coding the upper percentiles.

length indicates that the following facial regions, with descriptions given for increasing 'femaleness', are of particular importance in sexual dimorphism:

1 Upper lip and philtrum: this area is displaced posteriorly and superiorly; it reduces in area, particularly medially.

2 Nose: this narrows along its length, reduces in area and is displaced posteriorly; the tip of the nose moves posteriorly so the nose becomes relatively shorter; its anterior extent is displaced superiorly leading to a turning up of the tip of the nose.

3 Cheeks: these expand in area and are displaced outwards.

4 Chin and mandible: the chin reduces in area and is displaced superiorly and posteriorly; the angle of the mandible is displaced medially; the mandible is reduced in relative length.

5 Superior and inferior ear attachments: the inferior attachment is displaced medially whereas the superior attachment is displaced inferiorly. The overall effect is a rotation of this area in the coronal plane.

6 Orbital margins: the superior medial orbital margins are displaced superiorly and posteriorly whereas the superior lateral margins are displaced laterally; the lateral margins are displaced laterally.

7 Forehead: the medial forehead is displaced anteriorly and expands laterally; the lateral aspects are displaced anteriorly without lateral expansion.

On comparison of the surface analysis in Fig. 4 with our previous 24-landmark analysis (Hennessy et al. 2002), it is clear that, although the results are consistent, the surface analysis contains strikingly more anatomical information. Large areas of the face are analysed that are not recorded by landmarks; the cheeks, jaw, orbits and forehead are important examples. Even areas of the face that are located by the landmarks – mouth, nose, chin, eyes – are much more convincingly imaged as surfaces. In addition, the dynamic 3D graphics enables the discrimination to be viewed as a warping of a recognizable face. This demonstrates that the specific anatomical features identified quantitatively by visualization of the logistic regression model elaborate general, qualitative understanding of sexually dimorphic features (Enlow & Hans, 1996).

Ordination

The coefficients for correlations between the linear discriminant function scores for the highest resolution

surface and each of the other surfaces are plotted in Fig. 3. It is apparent that the ordinations are closely similar as long as the mean intervertex distance is less than ~13 mm, i.e. surfaces have more than ~200 co-ordinates. This suggests that the scale of the features responsible for the ordination is less than ~13 mm. Inspection of Fig. 2 suggests that these features are, primarily, the mouth and nose. The substantial difference in ordination for the 24-landmark analysis is largely due to the important anatomical features that are not captured by these 24 landmarks.

Methodological approaches: morphological–functional relationships

Cognitive measures

Cognitive testing was conducted on the above subjects blind to facial shape analysis (see Hennessy et al. 2005). Subjects were assessed using: (i) Trail Making Tests A and B, tests of spatial attention, visuomotor tracking and processing speed (Reitan & Wolfson, 1985) – the mean time to complete Test A was 27.9 s (SD 7.4) in men and 27.0 s (SD 6.0) in women, while the mean time to complete Test B was 54.5 s (SD 12.9) in men and 51.5 s (SD 12.4) in women; and (ii) the Controlled Oral Word Association Test, a test of verbal fluency (Benton & Hamsher, 1976) – the mean production/3 min was 45.7 words (SD 18.8) in men and 44.1 words (SD 14.2) in women.

Covariance of cognitive measures with facial surface shape

The high-resolution surfaces with ~1700 vertices were used for this study as the results reported above indicate indistinguishable analytical results for all the higher resolution pseudo-landmark sets.

The methodology described above was used to generate pseudo-landmark sets and to calculate PCs of shape. Multiple linear regression of cognitive measures onto shape PCs was then used to determine significant PCs. Because cognitive measures correlate with age, age was added to the independent variables and PCs were only included in the model if they retained their significance on controlling for age; R^2, F and P values for the models were recorded.

In order to visualize the models, multivariate regression of significant shape PCs onto cognitive measures was used to generate β coefficients as described above.

Morphological–functional relationships

Facial shape covaried with cognitive performance in a sexually dimorphic manner. Among men, the regression model for time to complete Trail Making Test A was associated with one PC of facial shape, which explains 14% of the variance in completion time ($F = 6.21$, d.f. = 1, $P < 0.05$); on visualization of this statistical model (Fig. 6), increasing spatial attention, visuomotor tracking and processing speed was associated primarily with a relative increase in anterior–posterior length and relative decrease in facial width. Time to complete Trail Making Test B, which places additional demands on attention and 'set shifting' relative to Test A, was associated with one PC of facial shape, which explains 22% of the variance in completion time ($F = 10.13$, d.f. = 1, $P < 0.005$); on visualization of this statistical model (Fig. 6), increasing spatial attention, visuomotor tracking, processing speed and 'set shifting' was associated primarily with anterior displacement of chin, posterior displacement of mouth, narrowing of cheeks and anterior displacement of forehead. Conversely, verbal fluency was unrelated to any component of facial shape in men.

In women, times to complete Trail Making Tests A and B were not associated with any PC of facial shape. Conversely, the regression model for verbal fluency score was associated with two PCs of facial shape in women, which explain 16% of the variance in verbal fluency score ($F = 5.86$, d.f. = 2, $P < 0.005$); on visualization of this statistical model (Fig. 6), increasing verbal fluency was associated primarily with anterior–inferior displacement of the nose, anterior–superior displacement of the chin, inferior displacement of the upper lip, inward displacement of the cheeks, posterior–superior displacement of the forehead and relative widening of the lateral face.

This pattern of sexual dimorphism in covariance of facial shape with cognitive performance is consistent with but elaborates in considerably greater detail that found in our previous 24-landmark analysis (Hennessy et al. 2005).

Conclusions

This article concerns capturing the facial surface in three dimensions, analysing these surfaces using geometric morphometrics on a 'whole-face' basis and visualizing anatomically the statistical models. The

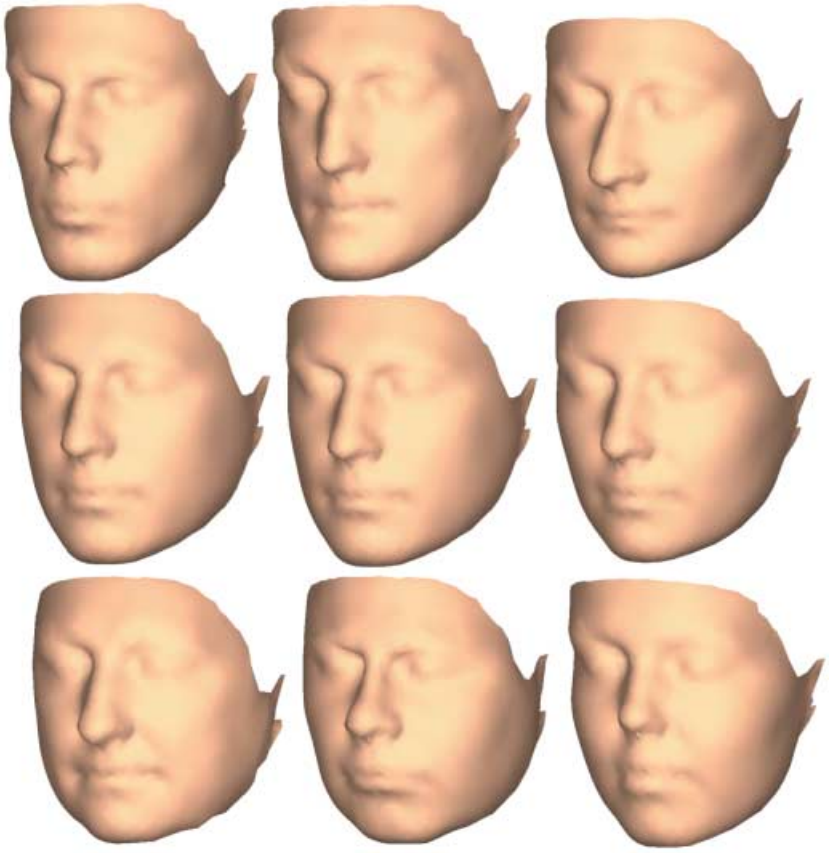

Fig. 6 Covariance of facial shape with cognitive measures. The upper row shows facial shape corresponding to improvement in cognitive performance score by 10 SDs, i.e. 74 s in Trail Making Test A score for males (left column), 129 s in Trail Making Test B score for males (middle column) and 142 words in verbal fluency score for females (right column). The middle row shows the Procrustes means. The lower row shows facial shape corresponding to disimprovement in cognitive performance score by 10 SDs.

rationale for this work (see Introduction) is: (i) the intimate embryological relationship between the face and brain such that facial dysmorphogenesis can be an accessible and informative index of brain dysmorphogenesis in neurological and psychiatric disorders of early developmental origin; (ii) the requirement to resolve, both statistically and anatomically, subtle quantitative differences between particular patient populations and controls; and (iii) the necessity to demonstrate a relationship between facial morphogenesis and brain morphogenesis not only in anatomical–embryological terms but also at the level of brain function.

Using 3D laser surface scanning (Hennessy et al. 2002), we have studied sexual dimorphism in human facial shape and its cognitive correlates as an exemplar for the technical and analytical challenges outlined above. Our analytical techniques elaborate the approaches of Hutton et al. (2003) and Hammond et al. (2004) for surface analysis on a 'whole-face' basis. We then apply our previously described (Hennessy et al. 2002, 2004) geometric morphometric approaches for statistical analysis and anatomical visualization of group differences. In elaboration of these, we describe new procedures for identifying statistically and visualizing anatomically those aspects of shape difference that particularly affect the group discrimination at issue, here sexual dimorphism in facial shape among the normal population.

Although the ability to discriminate subjectively the shape of the face as 'male' or 'female' underpins multiple aspects of human behaviour, the anatomical basis of this discrimination has received very little study at a quantitative level using shape space methods. In our initial study of sexual dimorphism in facial shape, using a 24-landmark approach (Hennessy et al. 2002), we described, for the first time, statistically significant features that distinguish male and female human faces. Here, the 'whole-face' analysis elaborates these findings by revealing numerous additional aspects of facial shape that remain undetected using the landmark-based approach; this attests critically to the value of 'whole-face' analysis for intergroup comparisons.

The domains of facial shape identified as distinguishing male and female faces have their origins in the interplay of general and sex-dependent developmental programmes, which arise over early fetal life, during

which craniofacial and cerebral morphogenesis constitute a unitary process (see Hennessy et al. 2002): there is initiation of the general developmental trajectory of the face and brain, which begins over weeks 6–9 of gestation in a manner independent of sex; subsequently, beginning with gonadal hormone secretion after week 10, hormones modulate this trajectory to result in sexual dimorphism both of the face and of the brain, such that morphogenesis proceeds in a primarily female fashion in the absence of gonadal hormone secretion after week 10 (Breedlove, 1992). This would be consistent with the features of increasing maleness identified above on 'whole-face' analysis having a substrate in the impact of such hormones to modulate this developmental programme.

More specifically, over the period from 6–9 weeks through to 16–19 weeks of fetal life there is a critical 3D trajectory of embryonic–fetal craniofacial development, particularly along the midline, during which there is: (i) vertical growth of the anterior mid-facial (frontonasal) region; (ii) narrowing of the frontonasal prominences; (iii) primary palate formation; (iv) dissociation of cranial base width from anterior facial changes; and (v) vertical separation of the brain and face, with the face growing forward more rapidly than is the brain (Diewert & Lozanoff, 1993a,b; Diewert et al. 1993; Kjaer, 1995; Waddington et al. 1999a,b; Lieberman et al. 2000a,b; Cohen 2002; Hennessy et al. 2002; Baldwin et al. 2004); thereafter, the craniofacies continue to evolve over later gestation, infancy, childhood and adolescence, particularly in terms of overall growth, to attain adult form (Enlow & Hans, 1996; Hennessy et al. 2002).

In accordance with emergent understanding of general 3D regulation of development (Hao et al. 2001), there is now recognized to be an exquisite embryological intimacy with which morphogenesis of the frontonasal prominences, forebrain and anterior midline regions are regulated via epithelial–mesenchymal signalling interactions; for example, rather than previous notions of the face developing on a cerebral scaffold, the neural crest, neuroepithelium, nascent forebrain and especially facial ectoderm, from which the present soft tissue measurements derive, function as a developmental unit in terms of 3D gene expression domains (Diewert & Lozanoff, 1993a,b; Diewert et al. 1993; Kjaer, 1995; Schneider et al. 2001), with posterior craniofacial and cerebral development being related less intimately and regulated by alternative mechanisms (Kjaer, 1995; Brault et al. 2001; Wilkie & Morriss-Kay, 2001). Our 'whole-face' analysis appears to be quantifying sexual dimorphism in these processes and visualizing their consequences in adulthood.

It is on these anatomical–embryological grounds that the present technology and morphometric approach to facial shape analysis appears to have *prima-facia* merit for accessing cerebral (dys)morphogenesis through facial (dys)morphogenesis. However, there remains at least one additional challenge: to what extent does adult facial shape, through facial morphogenesis, reflect not only brain morphogenesis but also brain function? We have previously presented preliminary findings, using a landmark-based approach, that facial shape covaries with cognitive function in a sexually dimorphic manner (Hennessy et al. 2005). Here we extend these analyses to specify the domains of facial shape variation that mediate these relationships.

It is important to emphasize firstly that the magnitude of variation in facial shape variation that is associated with variation in cognitive performance is unlikely to be observed qualitatively in any individual by another individual. However, using 3D laser surface scanning and geometric morphometrics on a 'whole-face' basis, double dissociations were consistently found: the shape of the anterior face co-varied with spatial attention, visuomotor tracking and processing speed in men but not in women, and with verbal fluency in women but not in men. These facial findings relating to the face complement general findings relating to the brain, in that the sexes differ in cerebral morphology (Gur et al. 1999; Goldstein et al. 2001) and cognitive abilities (Caplan et al. 1997; Gur et al. 1999). It is striking that the present dissociations in relation to facial morphology involve for each sex the cognitive domain in which that sex shows, at least in large samples, preferential overall performance: in general, men perform better than women on visuospatial tasks, whereas women perform better than men on verbal tasks (Caplan et al. 1997; Gur et al. 1999).

In addition, the present sexual dimorphism in correlations of facial shape domains with cognitive measures is notably similar to reported correlations between brain structural volumes on MRI and IQ in normal individuals (Andreasen et al. 1993): in women, verbal IQ was found to correlate with the majority of brain structures examined (cranium, left and right cerebrum, left and right temporal lobes, cerebellum and left and right hippocampus) while the correlations with performance

IQ were much reduced; for men, the majority of the correlations were with performance IQ (cranium, left cerebrum, cerebellum and left hippocampus). Thus, when juxtaposed with anatomical–embryological considerations, the present relationships between facial shape domains and cognitive measures constitute strong evidence that facial morphogenesis is an index not only of brain morphogenesis but also of associated brain function.

Schizophrenia is a disorder for which there is much epidemiological but considerably less 'hard' biological evidence for a basis in disruption to early brain development (Waddington et al. 1999a; Baldwin et al. 2004). We (Lane et al. 1997) and others (McGrath et al. 2002) have reported craniofacial dysmorphogenesis in schizophrenia using classical anthropometric techniques. Recently, we have conducted a preliminary study of simple 3D configurations from the unique subset of linear anthropometric measurements that define the unambiguous space encompassed by those measurements and find them to distinguish patients with schizophrenia from controls (Hennessy et al. 2004). However, these utilize only a very limited amount of anatomical information. Therefore, given that the present studies indicate the sensitivity, incisiveness and biological significance of facial (dys)morphogenesis for informing on brain (dys)morphogenesis, we are acquiring extensive 3D laser surface scanning data in patients with schizophrenia in comparison with controls. Application of geometric morphometrics on a 'whole-face' basis may confer sufficient power to detect and resolve in schizophrenia dysmorphology more subtle than that characterizing sexual dimorphism. These approaches can, of course, be applied to any CNS disorder of putative early developmental origin.

Acknowledgements

These studies were supported by the Stanley Medical Research Institute under the Programme for Human Genomics of the Higher Education Authority's Programme for Research in Third Level Institutions.

References

Allanson JE, O'Hara P, Farkas LG, Nair RC (1993) Anthropometric craniofacial profiles in Down syndrome. *Am J Med Genet* **47**, 748–752.

Andreasen NC, Flaum M, Swayze V, et al. (1993) Intelligence and brain structure in normal individuals. *Am J Psychiatry* **150**, 130–134.

Baldwin P, Hennessy RJ, Morgan MG, Quinn JF, Scully PJ, Waddington JL (2004) Controversies in schizophrenia research: the 'continuum' challenge, heterogeneity vs homogeneity, and lifetime developmental-'neuroprogressive' trajectory. In *Search for the Causes of Schizophrenia* (eds Gattaz W, Haffner H, 394–409). Darmstadt: Steinkopff.

Benton A, Hamsher K (1976) *Multilingual Aphasia Examination*. Iowa City: University of Iowa Press.

Bookstein FL (1997a) Shape and the information in medical images: a decade of the morphometric synthesis. *Comput Vis Image Understand* **66**, 97–118.

Bookstein FL (1997b) Landmark methods for forms without landmarks: morphometrics of group difference in outline shape. *Med Image Anal* **1**, 225–243.

Bookstein FL, Schäfer K, Prossinger H, et al. (1999) Comparing frontal cranial profiles in archaic and modern *Homo* by morphometric analysis. *Anat Rec* **257**, 217–224.

Bookstein FL, Sampson PD, Streissguth AP, Connor PD (2001) Geometric morphometrics of corpus callosum and subcortical structures in the fetal-alcohol affected brain. *Teratology* **64**, 4–32.

Brault V, Moore R, Kutsch S, et al. (2001) Inactivation of the beta-catenin gene by Wnt 1-Cre mediated deletion results in dramatic brain malformation and failure of craniofacial development. *Development* **128**, 1253–1264.

Breedlove SM (1992) Sexual dimorphism in the vertebrate nervous system. *J Neurosci* **12**, 4133–4142.

Buckley PF, Dean D, Bookstein FL, et al. (1999) Three-dimensional magnetic resonance-based morphometrics and ventricular dysmorphology in schizophrenia. *Biol Psychiatry* **45**, 62–27.

Caplan PJ, Crawford M, Hyde JS, Richardson JTE (1997) *Gender Differences in Human Cognition*. New York: Oxford University Press.

Cohen MM (2002) Malformations of the craniofacial region. *Am J Med Genet* **115**, 245–268.

Dean D, Hans MG, Bookstein FL, Subramanyan K (2000) Three-dimensional Bolton–Brush growth study landmark data: ontogeny and sexual dimorphism of the Bolton standards cohort. *Cleft Pal Craniofac J* **37**, 145–156.

DeQuardo JR, Bookstein FL, Green WDK, Brunberg JA, Tandon R (1996) Spatial relationships of neuroanatomical landmarks in schizophrenia. *Psychiat Res Neuroimaging* **67**, 81–95.

Diewert VM, Lozanoff S (1993a) A morphometric analysis of human embryonic craniofacial growth in the median plane during primary palate formation. *J Craniofac Genet Dev Biol* **13**, 147–161.

Diewert VM, Lozanoff S (1993b) Growth and morphogenesis of the human embryonic midface during primary palate formation analyzed in frontal sections. *J Craniofac Genet Dev Biol* **13**, 162–183.

Diewert VM, Lozanoff S, Choy V (1993) Computer reconstructions of human embryonic craniofacial morphology showing changes in relations between the face and brain during primary palate formation. *J Craniofac Genet Dev Biol* **13**, 193–201.

Dryden I, Mardia K (1998) *Statistical Shape Analysis*. Chichester: Wiley.

Enlow DH, Hans MG (1996) *Essentials of Facial Growth*. Philadelphia: W.B. Saunders.

Gharaibeh WS, Rohlf FJ, Slice DE, DeLisi LE (2000) A geometric morphometric assessment of change in midline brain structural shape following a first episode of schizophrenia. *Biol Psychiatry* **48**, 398–405.

Goldstein JM, Seidman LJ, Horton NJ, et al. (2001) Normal sexual dimorphism of the adult human brain assessed by in-vivo magnetic resonance imaging. *Cerebral Cortex* **11**, 490–497.

Goodall CR (1991) Procrustes methods in the statistical analysis of shape. *J Roy Stat Soc* **B53**, 285–339.

Gur RC, Turetsky BI, Matsui M, et al. (1999) Sex differences in brain gray and white matter in healthy young adults: correlations with cognitive performance. *J Neurosci* **19**, 4065–4072.

Hammond P, Hutton TJ, Allanson JE, et al. (2004) 3D analysis of facial morphology. *Am J Med Genet* **126A**, 339–348.

Hao JC, Yu TW, Fujisawa K, et al. (2001) C. elegans slit acts in midline, dorsal-ventral, and anterior-posterior guidance via SAX-3/Robo receptor. *Neuron* **32**, 25–38.

Hennessy RJ, Moss JP (2001) Facial growth: separating shape from size. *Eur J Orthodont* **23**, 275–285.

Hennessy RJ, Kinsella A, Waddington JL (2002) 3D laser surface scanning and geometric morphometric analysis of craniofacial shape as an index of cerebro-craniofacial morphogenesis: initial application to sexual dimorphism. *Biol Psychiatry* **51**, 507–514.

Hennessy RJ, Stringer CB (2002) Geometric morphometric study of the regional variation of modern human craniofacial form. *Am J Phys Anthropol* **117**, 37–48.

Hennessy RJ, Lane A, Kinsella A, Larkin C, O'Callaghan E, Waddington JL (2004) 3D morphometrics of craniofacial dysmorphology reveals sex-specific asymmetries in schizophrenia. *Schizophr Res* **67**, 261–268.

Hennessy RJ, McLearie S, Kinsella A, Waddington JL (2005) Facial shape and asymmetry by 3D laser surface scanning covary with cognition in a sexually dimorphic manner. *J Neuropsychiat Clin Neurosci* in press.

Hill A, Cootes TF, Taylor CJ (1996) Active shape models and the shape approximation problem. *Image Vis Comput* **14**, 601–607.

Hutton TJ, Buxton BF, Hammond P, Potts HW (2003) Estimating average growth trajectories in shape-space using kernel smoothing. *IEEE Trans Med Imaging* **22**, 747–753.

Johnson RM (1963) On the theorem stated by Eckart and Young. *Psychometrika* **28**, 259–263.

Kjaer I (1995) Human prenatal craniofacial development related to brain development under normal and pathological conditions. *Acta Odontol Scand* **53**, 135–143.

Lane A, Larkin C, Waddington JL, O'Callaghan E (1996) Dysmorphic features and schizophrenia. In *The Neurodevelopmental Basis of Schizophrenia* (eds Waddington JL, Buckley PF), pp. 79–93. Georgetown: Landes.

Lane A, Kinsella A, Murphy P, et al. (1997) The anthropometric assessment of dysmorphic features in schizophrenia as an index of its developmental origins. *Psychol Med* **27**, 1155–1164.

Lieberman DE, Pearson OM, Mowbray KM (2000a) Basicranial influence on overall cranial shape. *J Hum Evol* **38**, 291–315.

Lieberman DE, Ross CF, Ravosa MJ (2000b) The primate cranial base: ontogeny, function and integration. *Yearb Phys Anthropol* **30**, 117–170.

McGrath JC, El-Saadi O, Grim V, et al. (2002) Minor physical anomalies and quantitative measures of the head and face in psychosis. *Arch Gen Psychiatry* **59**, 458–464.

Menard S (2000) Coefficients of determination for multiple regression analysis. *Am Stat* **54**, 17–24.

Murphy K, Owen MJ (2001) Velo–cardio–facial syndrome: a model for understanding the genetics and pathogenesis of schizophrenia. *Br J Psychiatry* **179**, 397–402.

Nopoulos P, Berg S, Canady J, Richman L, Van Demark D, Andreasen N (2002a) Structural brain abnormalities in adult males with clefts of the lip and/or palate. *Genet Med* **4**, 1–9.

Nopoulos P, Berg S, Van Demark D, Richman L, Canady J, Andreasen N (2002b) Cognitive dysfunction in adult males with non-syndromic clefts of the lip and/or palate. *Neuropsychologia* **40**, 2178–2184.

O'Higgins P, Jones N (1998) Facial growth in *Cercocebus torquatus*: an application of three-dimensional geometric morphometric techniques to the study of morphological variation. *J Anat* **193**, 251–272.

Penin X, Berge C, Baylac M (2002) Ontogenetic study of the skull in modern humans and the common chimpanzees: neotenic hypothesis reconsidered with a tridimensional Procrustes analysis. *Am J Phys Anthropol* **118**, 50–62.

Reitan RM, Wolfson D (1985) *The Halstead–Reitan Neuropsychological Test Battery: Theory and Clinical Interpretation*. Tucson, AZ: Neuropsychology Press.

Rohlf FJ (2000) Statistical power comparisons among alternative morphometric methods. *Am J Phys Anthropol* **111**, 463–478.

Schneider RA, Hu D, Rubenstein JLR, Maden M, Helms JA (2001) Local retinoid signaling coordinates forebrain and facial morphogenesis by maintaining FGF8 and SHH. *Development* **128**, 2755–2767.

Singh GD, McNamara JA, Lozanoff S (1997) Spline analysis of the mandible in human subjects with Class III malocclusion. *Arch Oral Biol* **5**, 345–353.

Tibbo P, Nopoulos P, Arndt S, Andreasen NC (1998) Corpus callosum shape and size in male patients with schizophrenia. *Biol Psychiatry* **44**, 405–412.

Waddington JL, Lane A, Larkin C, O'Callaghan E (1999a) The neurodevelopmental basis of schizophrenia: clinical clues from cerebro-craniofacial dysmorphogenesis, and the roots of a lifetime trajectory of disease. *Biol Psychiatry* **46**, 31–39.

Waddington JL, Lane A, Scully P, et al. (1999b) Early cerebro-craniofacial dysmorphogenesis in schizophrenia: a lifetime trajectory model from neurodevelopmental basis to 'neuroprogressive' process. *J Psychiat Res* **33**, 477–489.

Waldrop MF, Pedersen FA, Bell RQ (1968) Minor physical anomalies and behaviour in preschool children. *Child Devel* **39**, 391–400.

Weber GW, Schafer Prossinger H, Gunz P, Mitterocker P, Seidler H (2001) Virtual anthropology: the digital evolution in anthropological sciences. *J Physiol Anthropol* **20**, 69–80.

Wilkie AO, Morriss-Kay J (2001) Genetics of craniofacial development and malformation. *Nature Rev Genet* **2**, 458–468.